

# New insight into molecular interaction of heavy metal pollutant—cadmium(II) with human serum albumin

Yán Liu · Mingmao Chen · Longguang Jiang · Ling Song

Received: 2 December 2013 / Accepted: 27 January 2014 / Published online: 14 February 2014  
© Springer-Verlag Berlin Heidelberg 2014

**Abstract** Cadmium (Cd) is an extremely toxic metal commonly found as an environmental contaminant from industrial and agricultural sources, posing severe risks to human health. In this study, the binding mechanism of Cd(II)–human serum albumin (HSA) complex and the effect of Cd(II) on the conformational stability and structural state of HSA were comprehensively investigated through a series of efficient and appropriate methods. X-ray photoelectron spectroscopy accurately described the microenvironmental changes around protein C, N, and O atoms in the presence of Cd(II). Fluorescence results indicated that the probable mechanism of Cd(II)–HSA interaction is a static quenching process. Fourier transform infrared spectroscopy and dynamic light scattering showed Cd(II) complexation altered HSA conformation and the microenvironments of Trp and Tyr residues, accompanied by the size increases of HSA aggregates. This research will be helpful for understanding the toxic effects of Cd(II) on protein function *in vivo*.

**Keywords** Cadmium ion · Human serum albumin · Binding behavior · Secondary structure · Aggregation state · Spectroscopic methods

Responsible editor: Philippe Garrigues

Y. Liu · L. Jiang · L. Song (✉)  
The State Key Lab of Structural Chemistry, Fujian Institute of  
Research on the Structure of Matter, Chinese Academy of Sciences,  
Fuzhou, Fujian 350002, People's Republic of China  
e-mail: songling@fjirsm.ac.cn

M. Chen  
Institute of Biomedical and Pharmaceutical Technology, Fuzhou  
University, Fuzhou, Fujian 350002, People's Republic of China

## Introduction

Cadmium (Cd), belonging to group IIB of the periodic table of elements, is a potent environmental toxin that is present in measurable amounts in almost everything that we eat, drink, and breathe due to the widespread nature of its occurrence (Flick et al. 1971; Godt et al. 2006). This heavy metal pollutant has been demonstrated to have numerous undesirable effects on health in experimental animals and humans, targeting the kidneys, liver, and vascular systems in particular (Friberg 1984; Godt et al. 2006; Yang et al. 2013). It has been reported that occupational exposure to Cd(II) compounds in a number of industries, such as electronic components, electroplating, metal mechanic processing, and mining (Haddam et al. 2011; Haq et al. 1999), has been associated with increased risk of pathological cancer of the lung, kidney, and liver (Feki-Tounsi et al. 2013; Reshetin et al. 2003). In the blood circulation system, about 90 % of Cd(II) is bound to serum albumin and  $\alpha_2$ -macroglobulin, and Cd(II) bound to albumin is readily exchangeable (Scott and Bradwell 1983). In addition, Cd(II) contamination also causes metabolism problems in microorganisms (Heo et al. 2010; Mclamore et al. 2010). Due to its toxic characteristics, wastes from industrial processing of cadmium products are usually requested to be displaced properly in order to avoid the environment contamination (Mockaitis et al. 2012). Plants may contain certain amounts Cd through taking up Cd-contaminated water (Dudka and Adriano 1997). For human beings, Cd(II) has probably no biological function and could infiltrate into organisms through the respiratory tract and skin and then damage tissues and organs owing to its interactions with biological macromolecules (Nursita et al. 2009). People are exposed to Cd upon consumption of Cd containing plants or animals (Hallenbeck 1984). As a widely used pigment, Cd can also be found in plastic toys and food containers (Kumar and Pastore 2007). Even though the deadly effects of Cd(II) on

human health have been known for many years, the molecular mechanism of Cd(II) toxicity is poorly understood. Therefore, in order to better understand the toxic effects of Cd(II) on human health, it is necessary to elucidate the ion–protein interaction mechanism and the toxicological action of Cd(II) at molecular level.

Serum albumins (SAs) are the major soluble plasma proteins of the blood circulatory system *in vivo*, which is the most common media for transporting heavy metal ions and also has the capability to bind a wide range of endogenous and exogenous compounds (Carter and Ho 1994; Peters 1985). As a kind of serum albumin, human serum albumin (HSA) is a single-chain transporting protein of 585 amino acids with 17 tyrosine residues and only one tryptophanes located in position 214 (Curry et al. 1998; Sudlow et al. 1975), which is the ligand carrier's protein in blood serum and serves to amplify the capacity of plasma for transporting small molecules, such as drugs, fatty acids, hormones, and environmental toxicants (He and Carter 1992; Kamal et al. 2004). On the other hand, it has been demonstrated that the conformation of plasma protein can be changed by interaction with exogenous toxicants, which may influence protein's biological function as a carrier protein (Chi and Liu 2011; Ding et al. 2011). Therefore, the studies of binding of toxic Cd(II) to plasma proteins not only are helpful for understanding the metabolism and distribution of this toxicant *in vivo* but also can further elaborate the toxic effects of Cd(II) on protein function during the blood transportation process.

Because SA is one of the major binding proteins with cadmium in human body, several studies on the complexation of Cd(II) to SA have been reported in response to the increased demand for detection and study of adverse effect of cadmium ions in our body with various technologies, including equilibrium dialysis, radioactive-isotope dilution, isothermal microcalorimetry,  $^1\text{H}$  and  $^{113}\text{Cd}$  NMR, potentiometric titration, immunoabsorbent chromatography, and zone electrophoresis technologies (Perkins 1961; Qu et al. 2002; Rao and Lal 1958; Sadler and Viles 1996; Scott and Bradwell 1983). However, as one of widely used technologies for obtaining binding information between metal ions and macromolecules, spectroscopic methods have never been used to study the binding interaction of SA with Cd. Besides, since the range of symptoms of cadmium poisoning is so broad, no study on the conformational changes of SAs caused by interaction with Cd(II) has been reported. The exact molecular mechanism of cadmium poisoning is still unknown up to now.

In the present study, the binding characteristics of Cd(II) on HSA at the molecular level were systematically investigated by using X-ray photoelectron spectroscopy (XPS), fluorescence spectroscopy, Fourier transform infrared spectroscopy (FTIR), and dynamic light scattering (DLS) methods. The inner filter effect had been corrected before we estimated the Cd(II)–HSA binding information such as binding constants,

quenching rate constants, binding modes, binding sites, and intermolecular distances. The effects of Cd(II) on the micro-environment and conformation of HSA were also discussed. These results clarify the binding mechanism between Cd(II) and HSA, which is not only helpful for understanding the metabolism and distribution of this toxic metal ion *in vivo* but also can further elaborate the toxicological actions of Cd(II) on protein function during the blood transportation process.

## Experimental section

### Reagents

Human serum albumin, lyophilized and stored at 2–8 °C, was purchased from Sigma Chemical Co. and used as received. The cadmium nitrate, GR grade, was purchased from Merck. All other reagents of analytical grade were used. Double-distilled water with a resistivity of 18.2 M $\Omega$  (Milli-Q water, Millipore, USA) at room temperature (25 °C) was used throughout experiments. HSA was dissolved in 0.05 M phosphate-buffered saline solution to form an aqueous protein solution and then preserved at 4 °C for later use.

### Apparatus

XPS measurements were performed on an ESCALAB 250 X-ray photoelectron spectrometer (Thermo-VG Scientific Corporate, USA). Infrared spectra were recorded on a Spectrum One FTIR spectrometer (Perkin-Elmer Corporate, USA). Fluorescence data were obtained on a Cary Eclipse Spectrofluorometer (Varian Corporate, USA) equipped with 1.0 cm quartz cells. Dynamic light scattering measurements were done with a Nano ZS (model: ZEN3600, Malvern), employing a 5-mW, 633-nm He–Ne laser and equipped with a thermostated sample chamber. All pH measurements were conducted with a PHS-3C acidity meter.

### Methods

#### *Cd(II)–HSA complex formation*

Required amounts of HSA and cadmium nitrate solutions with/without further dilution are mixed together and kept aside for half an hour. Cd(II) ions attach to the electroactive sites of HSA forming a metal ion–protein complex.

#### *Spectroscopic characterizations*

XPS measurements were performed on an X-ray photoelectron spectrometer (ESCALAB 250, Thermo-VG Scientific Corporation) with amonochromatic focused Al K $\alpha$  X-ray source (1,486.6 eV) to determine C, N, and O on the sample

surface. Two 250  $\mu\text{M}$  of the sample were dropped on an aluminum substrate and dried in vacuum desiccator overnight to obtain a thin film. The dried sample was then transferred to the XPS sample holder. The pressure in the sample chamber was maintained at  $10^{-9}$  mbar. The detection was performed at  $45^\circ$  with respect to the sample surfaces. Thermo Avantage software was used for background subtraction, peak integration, fitting, and quantitative chemical analysis. Surface elemental stoichiometry was determined from peak–area ratio. For each sample, the analyses were made at three different points on the slices, and atomic fractions were calculated from averages of the three.

For the fluorescence measurement, Cd(II) solution was added into the protein solutions in sequence. Both Cd(II) and HSA concentrations were calculated by weight for consistency. The systems were excited at 280 nm, and the emission wavelength was adjusted from 300 to 500 nm with a scanning speed of  $600 \text{ nm min}^{-1}$ . The excitation and emission slit widths were both set at 5.0 nm. All the experiments were conducted in triplicate and further analyzed using Origin 8.0.

Time-resolved fluorescence spectra were executed in a time-correlated single photon counting system from FL920P spectrometer (Edinburgh Instruments, UK) with  $\lambda_{\text{ex}}=295 \text{ nm}$ . The data are fitted to biexponential functions after deconvolution of the instrumental response function by an iterative reconvolution approach by the DAS6 decay analysis software utilizing reduced  $\chi^2$  and weighted residuals as parameters for goodness of fit.

Molecular theoretical calculations were carried out using ICM (v3.4–8) software. The native structure of HSA (PDB ID 4IW2) was taken from Protein Data Bank with a crystalline resolution at 2.41 Å (Wang et al. 2013). All water molecules were removed, and local search was used to search for the optimum binding site of small molecules to the protein. A grid size of  $90 \times 90 \times 90$  points with a grid spacing of 0.4 Å was applied. The docking conformation with the lowest binding free energy was further processed by Pymol software.

For infrared spectra, the cadmium nitrate solution was added dropwise to the protein solution with constant stirring to ensure the formation of homogeneous solution and reach the target Cd concentrations of 2, 5, and 10 mM with a final protein concentration of 0.25 mM. Then, the sample solutions were placed between  $\text{CaF}_2$  windows separated with a 25- $\mu\text{M}$  spacer. Spectra were acquired at  $4 \text{ cm}^{-1}$  resolution and 100 scans.

The DLS experiments were carried out at 298 K with a Zetasizer Nano ZS (Malvern Instruments). The scattering intensity data were processed using the instrumental software to obtain the hydrodynamic diameter ( $d_{\text{H}}$ ) and the size distribution of the scatterer in each sample. The instrument measures the time-dependent fluctuation in the

intensity of light scattered from the particles in solution at a fixed scattering angle. Hydrodynamic diameter,  $d_{\text{H}}$ , is defined as,

$$d_{\text{H}} = k_{\text{B}}T / 3\pi\eta D$$

where  $k_{\text{B}}$  = Boltzmann constant,  $T$  = absolute temperature,  $\eta$  = viscosity coefficient of the solvent, and  $D$  = translational diffusion coefficient. Each measurement was performed on a freshly extracted aliquot of the protein sample and diluted with phosphate buffer to a final concentration of 10  $\mu\text{M}$  at different time intervals. All the experiments were conducted in triplicate and further analyzed using Origin 8.0 software.

## Results and discussion

### XPS study for Cd(II)–HSA complexation

To accurately investigate the binding interaction between Cd(II) and HSA at atomic level, we firstly applied XPS study. Figure 1 shows that the XPS spectrum of HSA only contains signals for the elements of C, N, and O, which are the main constituents of the amino acid residues and occur at 285, 400, and 532 eV, respectively. Figure 2 shows that HSA before and after the treatment with Cd(II) have different XPS C 1s core level spectra. The C 1s spectra can be deconvoluted into three components, which are attributed to carbon atom bound to carbon and hydrogen (C–C and C–H), carbon singly bound to nitrogen and oxygen (C–N and C–O), and carbon involved in an amide bond (O=C–NH), respectively (Belatik et al. 2012; Wu et al. 2009). The binding energies and C atomic fractions at different chemical states with and without Cd(II) are listed in Table 1. The intensities of the component located at around 284.6 and 285.8 eV changed obviously, which were probably coming from the complexation of Cd with carbon atoms and induced changes in the skeletal structure of protein. However, the intensity of the component located at 287.6 originating from the peptide bond almost had no change, implying that the primary structure of HSA had not yet been destroyed at the Cd(II) concentration = 0.25 mM. Figures 3 and 4 show the XPS signals attributed for N and O. The nitrogen component that bound to carbon (C–N) is located at 399.6 eV, and the other nitrogen component bound to hydrogen (N–H<sub>2</sub>) is located at 400.1 eV. The oxygen signals represented C=O and O–H are positioned at 531.2 and 532.3 eV, respectively. After the addition of Cd(II), the binding energy and atomic fraction values were changed, indicating the direct interaction between Cd and nitrogen, oxygen atoms. The major

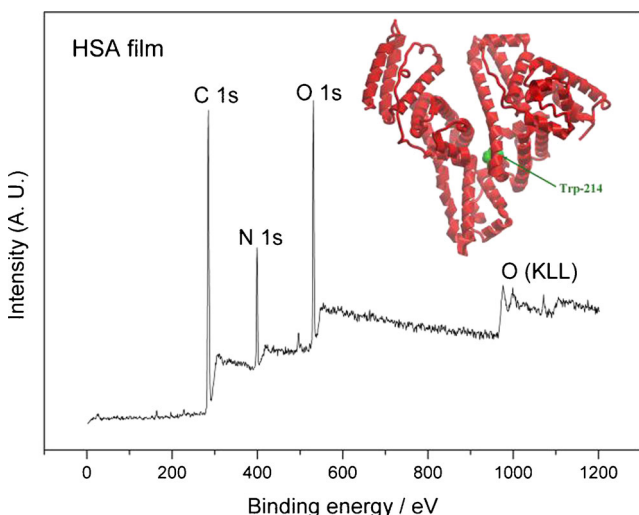


**Fig. 1** XPS survey spectrum for free HSA film (the main elements of C, N, and O are located at 285, 400, and 532 eV, respectively)

fraction and intensity changes observed for N and O were coming from direct Cd coordination with nitrogen and

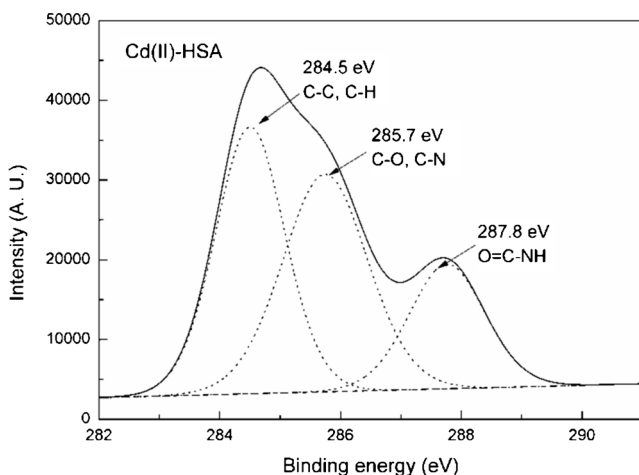
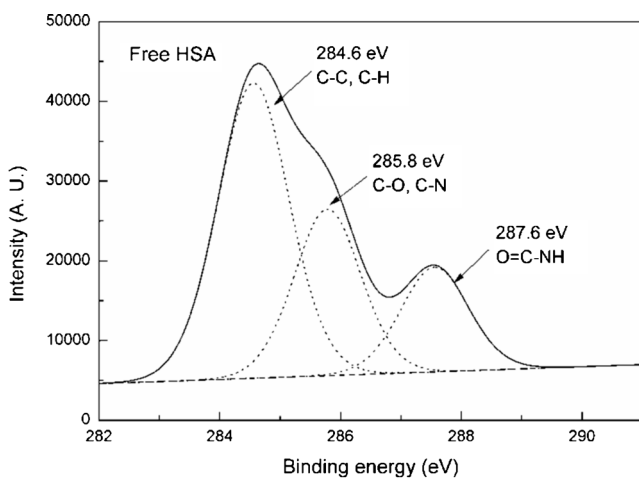


**Fig. 2** XPS spectra of C atom for the free HSA and Cd–HSA complex. Conditions: [HSA]=[Cd(II)]= $0.25 \times 10^{-3}$  mol L<sup>-1</sup>

oxygen atoms, which probably induced the formation of [Cd=O] and [Cd=N] units in the Cd–HSA complex.

Moreover, the experimental atomic composition as determined from the XPS spectral analysis was also calculated for nitrogen to carbon (N/C) and oxygen to carbon (O/C) ratios in the absence and presence of Cd(II). The values of N/C and O/C are 18.25 and 24.44 % without Cd(II), while the corresponding values increased to 19.24 and 28.06 % in the presence of Cd(II). The major ratio changes observed for N and O were coming from direct Cd coordination with nitrogen and oxygen atoms, while the alterations of C ratios were related to the linkage of C atom to metal ion-bonded N and O atoms. The XPS results show that the microenvironment around protein C, N, and O changes in the presence of Cd(II).

### Fluorescence spectra

#### Effect of Cd on the fluorescence spectra of HSA

Fluorescence quenching is a powerful tool to characterize the accessibility of fluorophores in the protein matrix to quenchers in solution. Detailed information of metal ions to protein such as the binding mode, binding constants, and conformational transformation can be obtained by the fluorescence technique (Lakowicz 2006). Herein, fluorescence quenching was utilized to study the interaction between Cd(II) and HSA.

Since the inner filter effect (IFE) may affect fluorescence measurements due to the formation of Cd(II)–HSA complex, we take advantage of some effective methods to correct the fluorescence of the complex and reduce the IFE. Firstly, each fluorescence spectrum of HSA in the presence of different concentrations of Cd(II) was corrected for any possible IFE using the following equation (Eq. 1) (Gu and Kenny 2009):

$$F_{cor} = F_{obs} 10^{\frac{A_{ex} \times d_{ex}}{2} + \frac{A_{em} \times d_{em}}{2}} \tag{1}$$

where  $F_{cor}$  is the corrected fluorescence intensity obtained in the absence of inner-filter effect,  $F_{obs}$  is the measured fluorescence, and  $A_{ex}$  and  $A_{em}$  are the sum of the absorbances of protein and ligand at the excitation and emission wavelengths, respectively, caused by ligand addition (in a  $1 \times 1$ -cm pathlength cuvette). Furthermore, in order to reduce as much as possible the inner filter effect caused by the absorption of both excitation radiation and emission radiation, we controlled the HSA concentration to be  $2.0 \times 10^{-6}$  mol L<sup>-1</sup> and the maximum concentration of Cd(II) to be  $1.0 \times 10^{-4}$  mol L<sup>-1</sup>. Thus, any possible contribution of

**Table 1** Binding energies and atomic fractions from the XPS spectra for C, N, and O elements in HSA in the absence and presence of Cd(II)

Subcomponents		Free HSA			Cd(II)–HSA complex		
		Binding energy (eV)	Atomic fractions (%)	Sum of each components	Binding energy (eV)	Atomic fractions (%)	Sum of each components
C(1s)	C–C and C–H	284.6	37.59	70.09	284.5	26.99	67.83
	C–N and C–O	285.8	19.80		285.7	27.01	
	O=C–NH	287.6	12.70		287.8	13.83	
N(1s)	C–N	399.6	10.77	12.79	399.6	6.31	13.05
	N–H <sub>2</sub>	400.1	2.02		399.9	6.74	
O(1s)	C=O	531.2	10.55	17.13	531.5	9.30	19.03
	O–H	532.3	6.58		532.4	9.74	

inner filter effect due to attenuation of the incident light by the quencher could be negligible. In addition, fluorescence backgrounds were also corrected for blank buffer solutions in each measurement.

As shown in Fig. 5a, free HSA gave a strong fluorescence emission band at 345 nm when excited at 280 nm, and free Cd(II) did not show any fluorescence emission under the same condition. The addition of Cd(II) led to a concentration-

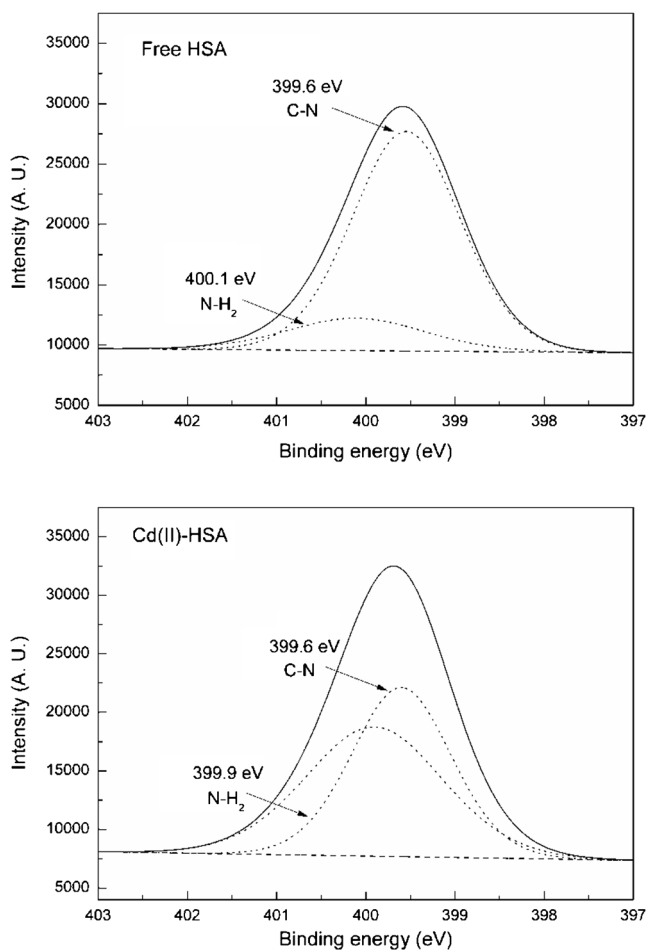


**Fig. 3** XPS spectra of N atom for the free HSA and Cd–HSA complex. Conditions: [HSA]=[Cd(II)]= $0.25 \times 10^{-3}$  mol L<sup>-1</sup>

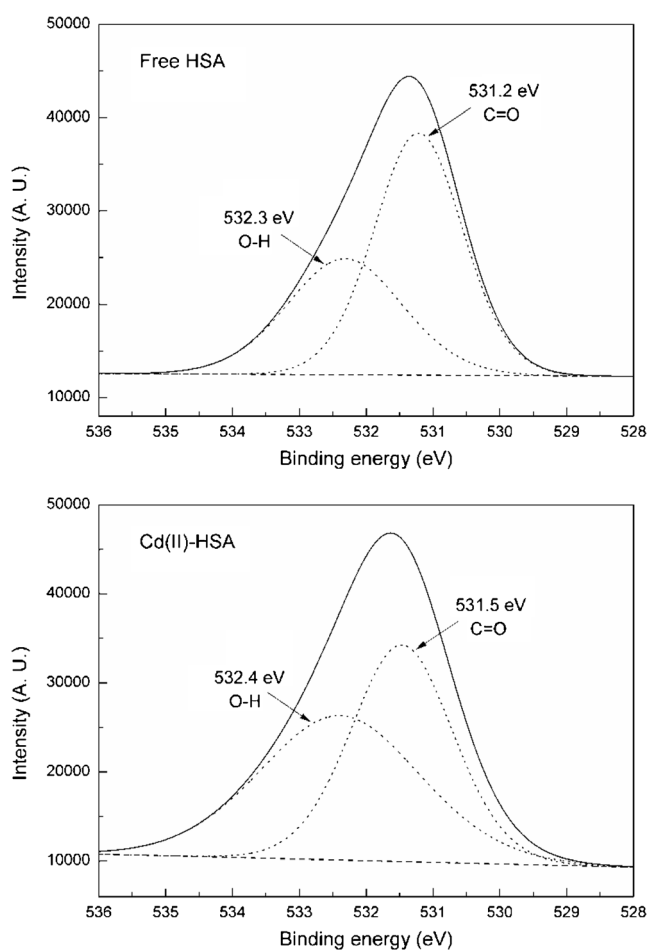


**Fig. 4** XPS spectra of O atom for the free HSA and Cd–HSA complex. Conditions: [HSA]=[Cd(II)]= $0.25 \times 10^{-3}$  mol L<sup>-1</sup>

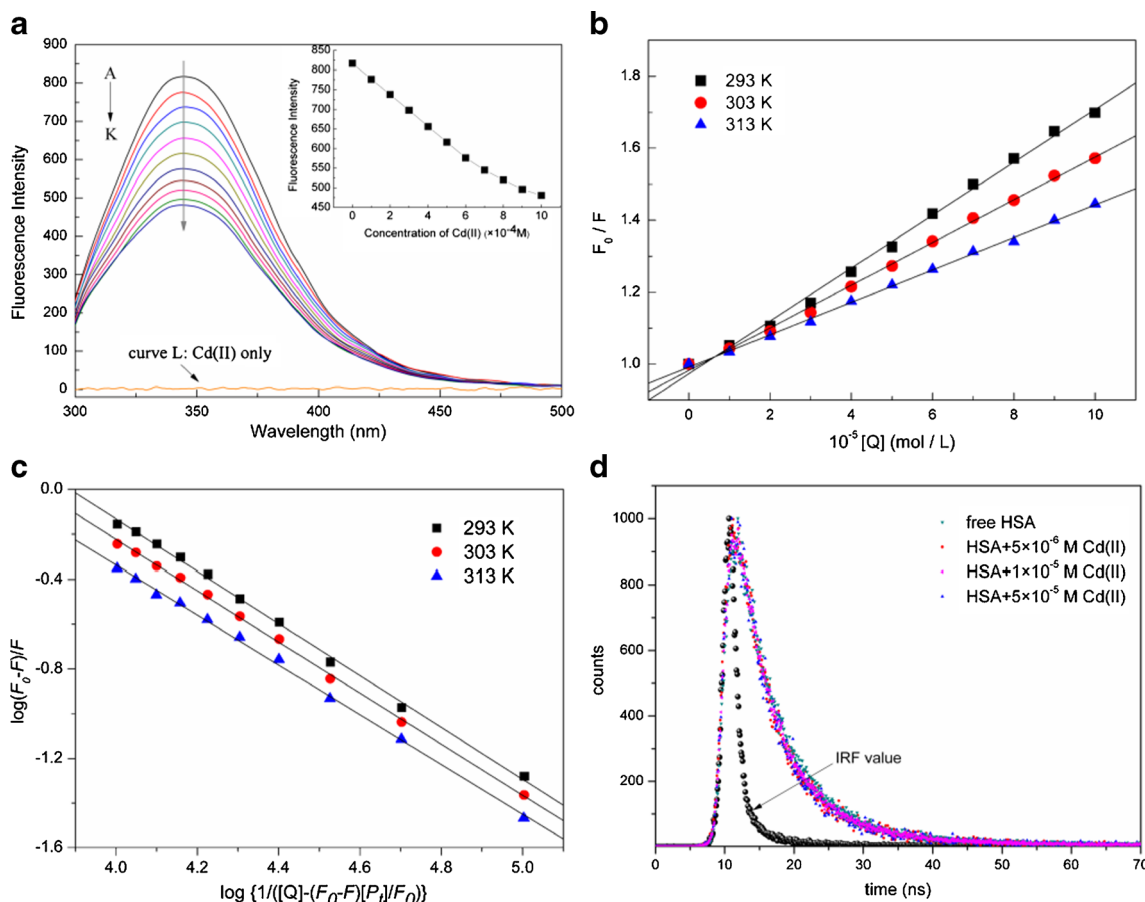


**Fig. 5** **a** Effect of Cd(II) on HSA fluorescence at 293 K. The *inset* shows the dependence of the fluorescence intensities of HSA by Cd(II) at corresponding concentrations; **b** Stern–Volmer plots for the fluorescence quenching of HSA by the addition of Cd(II); **c** plots of  $\log(F_0 - F)/F$  versus  $\log\{1/([Q] - (F_0 - F)P_q/F_0)\}$  for Cd(II)–HSA system at different

temperatures. Conditions:  $[HSA] = 2.0 \times 10^{-6} \text{ mol L}^{-1}$ ;  $[Cd(II)]$  (a–q) = 0, 1.0, 2.0, 3.0, 4.0, 5.0, 6.0, 7.0, 8.0, 9.0, and  $10.0 \times 10^{-4} \text{ mol L}^{-1}$ ; **d** The time-resolved fluorescence decay of  $1.0 \times 10^{-6} \text{ mol L}^{-1}$  HSA in the presence of Cd(II) with different concentrations

dependent quenching of the intrinsic fluorescence of HSA, and the wavelength emission maximum  $\lambda_{max}$  remained nearly unchanged in the HSA spectrum. HSA contains a single polypeptide of 585 amino acids with only one tryptophan (Trp-214) located in subdomain II A, and the Trp residue emission mainly dominates HSA fluorescence spectra in the UV region. The characteristic of the intrinsic fluorescence of HSA is very sensitive to its microenvironment, so changes in the intrinsic fluorescence of HSA can provide valuable information about its structure and dynamics. Therefore, the results imply that the binding of Cd(II) to HSA occurs and Cd(II) probably increases the exposure of the chromophore amino acids to the aqueous medium and therefore quench the intrinsic fluorescence of HSA.

*The fluorescence quenching mechanism*

Fluorescence quenching can occur in two different processes: static and dynamic quenchings (Lakowicz 2006). In this study,

both static and dynamic processes are described by the Stern–Volmer Eq. 2.

$$\frac{F_0}{F} = 1 + K_q\tau_0[Q] = 1 + K_{SV}[Q] \tag{2}$$

where  $F_0$  and  $F$  are the steady-state fluorescence intensities without and with quencher (ET), respectively;  $K_q$  is the quenching rate constant;  $K_{SV}$  is the Stern–Volmer quenching constant; and  $[Q]$  is the concentration of the quencher. Hence, Eq. 2 was applied to determine  $K_{SV}$  by linear regression of a plot of  $F_0/F$  against  $[Q]$ .

Figure 5b displays the Stern–Volmer plots of the quenching of HSA tryptophan residue fluorescence by Cd(II). The values of  $K_{SV}$  and  $K_q$  were further calculated and listed in Table 2. It shows that the Stern–Volmer plots are linear and the linearity does not affected by the increasing temperature. The linearity of the Stern–Volmer plots may indicate the existence of a single type of quenching, either static or dynamic. Table 2

**Table 2** Stern–Volmer quenching constants for the interaction of Cd(II) with HSA at various temperatures

pH	<i>T</i> (K)	$K_{sv}$ ( $\times 10^3$ L mol $^{-1}$ )	$K_q$ ( $\times 10^{11}$ L mol $^{-1}$ s $^{-1}$ )	<i>R</i>	SD
7.4	293	7.352	12.131	0.9957	0.0089
	303	5.931	9.786	0.9975	0.0056
	313	4.508	7.438	0.9914	0.0038

*R* correlation coefficient, *SD* standard deviation

showed that  $K_{SV}$  and  $K_q$  were inversely correlated with temperature, which indicated that the probable quenching mechanism of Cd(II)–HSA binding reaction might be initiated by complex formation rather than by dynamic collision (Liu et al. 2013a). Moreover, values for  $K_q$  are much greater than the maximum diffusion collision quenching rate constant of the biomolecule ( $2.0 \times 10^{10}$  M $^{-1}$  s $^{-1}$ ) (Lakowicz 2006); therefore, the static quenching could be the main mechanism of the fluorescence quenching of HSA by Cd(II).

In addition, static quenching can easily be distinguished from that of dynamic preferably by lifetime measurements (Ware 1975). In this study, we used the lifetime measurements to confirm the quenching mechanism as static. Figure 5d exhibits the fluorescence decay of HSA in the absence and presence of Cd(II). The results show that Cd(II) with increasing concentrations had no effect in the lifetime of HSA, which reveals that the quenching mentioned above is not initiated by dynamic collision but from the ground state complex formation of static quenching.

#### Binding constants and number of binding sites

The static mechanism is principally responsible for the observed fluorescence quenching when Cd(II) binds to HSA as discussed above. In order to investigate equilibrium between free and bound molecules and rationalize our experimental data on the Cd(II)–HSA systems, the following equation has been employed (Eq. 3) (Mandal and Ganguly 2009):

$$\log \frac{F_0 - F}{F} = n \times \log K_a - n \times \log \frac{1}{[Q] - \frac{F_0 - F}{F_0} \times [P_t]} \quad (3)$$

where  $F_0$  and  $F$  are the fluorescence intensities before and after the addition of the quencher,  $K_a$  is the apparent binding constant, and  $n$  is the average number of binding sites per Hb;  $[Q]$  is the total ligand concentration, and  $[P_t]$  are the total protein concentration. By using Eq. 3, the values of  $K_a$  and  $n$  at physiological pH 7.4 can be calculated. Figure 5c is the plots of  $\log (F_0 - F)/F$  versus  $\log (1/([Q] - (F_0 - F) \times [P_t]/F_0))$  for the Cd(II)–HSA system at different temperatures, and the linearities are very well fitted with all  $R$  value  $> 0.99$ . The binding constant is  $7.692 \times 10^3$ ,  $6.385 \times 10^3$ , and  $4.988 \times$

$10^3$  L mol $^{-1}$ , and the number of binding sites is 1.161, 1.142, and 1.114 at 293, 303, and 313 K, respectively. The results showed that the binding constants  $K_a$  and binding sites  $n$  were decreased with increasing temperature, which may suggest that Cd(II) is partially dissociated from HSA as temperature increases. The number of binding sites  $n$  approximately equals 1, indicating that there is one binding site with higher binding affinity and selectivity in HSA for Cd(II) during their binding process.

#### Thermodynamic parameters

Generally, the binding forces between ligands and biomolecules may comprise hydrogen bonds, electrostatic forces, van der Waals forces, hydrophobic interactions, etc. (Gautier et al. 2008). The thermodynamic parameters, enthalpy change ( $\Delta H$ ), free-energy change ( $\Delta G$ ), and the entropy change ( $\Delta S$ ) are the main evidences for confirming binding modes and could be calculated according to the van't Hoff equation (Eq. 4) (Ross and Subramanian 1981):

$$\ln K_a = -\frac{\Delta H}{RT} + \frac{\Delta S}{R} \quad (4)$$

where  $K_a$  is analogous to the associative binding constants at the corresponding temperature and  $R$  is the gas constant. To elucidate the interaction between Cd(II) and HSA, the thermodynamic parameters can be calculated from the van't Hoff plots.  $\Delta G$  can then be estimated from the following relationship (Eq. 5):

$$\Delta G = \Delta H - T\Delta S = -RT \ln K_a \quad (5)$$

The main binding forces can be judged by thermodynamic parameters. From the viewpoint of thermodynamics,  $\Delta H > 0$  and  $\Delta S > 0$  imply that hydrophobic interaction is the main force;  $\Delta H < 0$  and  $\Delta S < 0$  reflect van der Waals force or hydrogen bonding;  $\Delta H < 0$  and  $\Delta S > 0$  suggest that electrostatic forces play a key role (Kumar et al. 2002). On account of the little temperature effect,  $\Delta H$  can be regarded as a constant if the temperature range is not too wide. The plots of  $\ln K_a$  versus  $1/T$  are presented in Fig. 6 and show a good linear relationship. The calculated thermodynamic parameters and

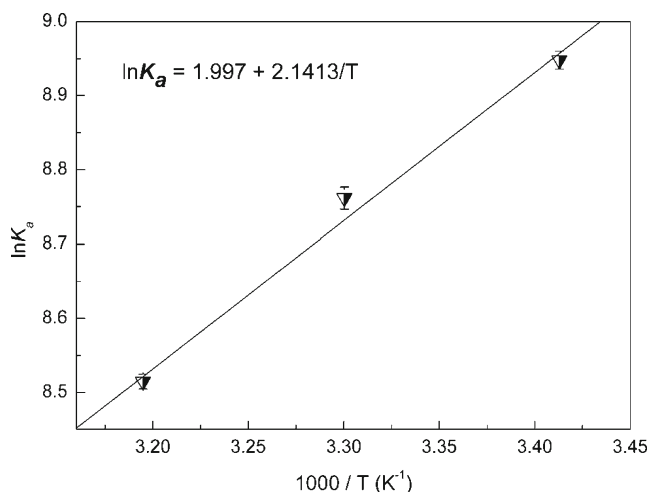


**Fig. 6** Plots of the van't Hoff equation of Cd(II)–HSA system at different temperatures

$K_a$  values for the binding interaction between Cd(II) and HSA are listed in Table 3. The corresponding negative  $\Delta H$  and positive  $\Delta S$  suggest that Cd(II) itself carries a positive charge and HSA carries negative charge in aqueous solution at physiological pH; therefore, the electrostatic forces play a major role in the formation of Cd(II)–HSA complex.

To further define the binding site, computational molecular docking was employed to improve the understanding of the interaction between Cd(II) and HSA. The best energy ranked result is shown in Fig. 7, and the geometry exhibits the lowest free energy. The docking result shows that Cd(II) mainly interacts with the negatively charged amino acid residues Asp451, Pro447, and Gln 221 predominately through electrostatic force, in agreement with the conclusion of thermodynamic analysis. The van der Waals interactions and some other forces might also exist between Cd(II) and HSA, but are not dominating. In addition, the formation of Cd(II)–HSA complex might give rise to a perturbation in the corresponding subdomain and then induce the structural alteration of HSA and microenvironment changes of Trp and Tyr, which could be reflected in the fluorescence intensity changes (Liu et al. 2013b).

Investigation on secondary structural changes of HSA

FTIR spectroscopy has been widely applied to monitor the conformational changes of proteins that spans different

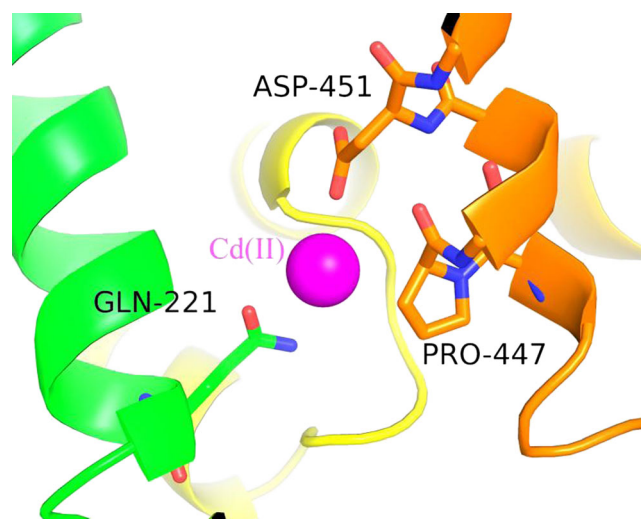


**Fig. 7** Molecular modeling of the interaction between Cd(II) and HSA. HSA is shown in *cartoon*. Cd(II) is represented using a *purple* sphere

secondary structures such as  $\alpha$ -helix (1,650–1,660  $\text{cm}^{-1}$ ),  $\beta$ -sheet (1,610–1,640  $\text{cm}^{-1}$ ), turn structure (1,660–1,680  $\text{cm}^{-1}$ ),  $\beta$ -antiparallel (1,680–1,692  $\text{cm}^{-1}$ ), and random coil (1,641–1,648  $\text{cm}^{-1}$ ) (Mantsch and Chapman 1996). The infrared spectra of proteins are mainly comprised of amide I (1,600–1,700  $\text{cm}^{-1}$ ) and amide II (1,500–1,600  $\text{cm}^{-1}$ ), which are caused by the carbonyl stretching vibrations of the peptide backbone (amide I band) and the combination of N–H in-plane bending and C–N stretching vibrations of peptide groups (amide II band) (Kong and Yu 2007; Mantsch and Chapman 1996). Herein, the interaction between Cd(II) and HSA was characterized by infrared spectroscopy and its derivative methods. The difference spectra [(protein+Cd solution)–(buffer solution)] were obtained. Figure 8 shows that an intense band in the amide I region centered at 1,655  $\text{cm}^{-1}$  could be observed in the original FTIR spectra of native HSA without Cd (II) at pH=7.4, indicating that HSA is in an  $\alpha$ -helix-rich conformation. As compared with that for the native HSA, the band in the Cd(II)–HSA complex system showed obvious changes in both shape and peak position (1,655–1,651  $\text{cm}^{-1}$ ). The spectral shift for the amide I from 1,655 to 1,651  $\text{cm}^{-1}$  in the spectra of Cd(II)–HSA complexes was due to the binding of Cd cation to protein C=O and C–N groups. In the presence of Cd(II), an increase in FTIR intensity was observed for the HSA amide I band, which was probably due to metal ion binding to protein C=O, C–N, and N–H

**Table 3** Binding constants and relative thermodynamic parameters of Cd(II) to HSA at different temperatures

$T$ (K)	$K_a$ ( $\times 10^3$ L mol $^{-1}$ )	$n$	$R^a$	$\Delta H$ (kJ mol $^{-1}$ )	$\Delta S$ (J mol $^{-1}$ K $^{-1}$ )	$\Delta G$ (kJ mol $^{-1}$ )
293	7.692	1.161	0.9977			–21.797
303	6.385	1.142	0.9986	–17.803	16.603	–22.072
313	4.988	1.114	0.9971			–22.158

<sup>a</sup>  $R$  is the correlation coefficient for the  $K_a$  values



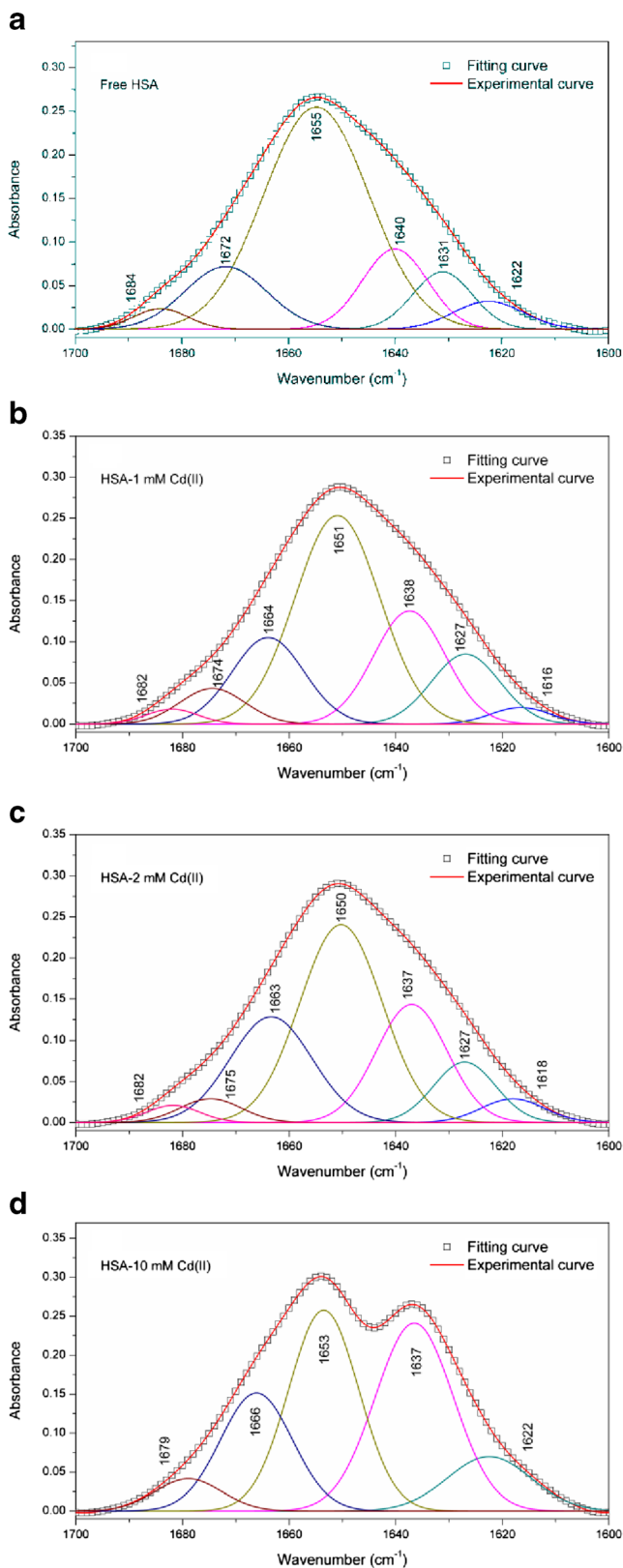


**Fig. 8** Second derivative resolution enhancement and curve-fitted amide I region ( $1,700\text{--}1,600\text{ cm}^{-1}$ ) for HSA in the absence (a) and presence Cd(II) adducts (b–d) with 1, 2, and 10 mM metal ion and 0.2 mM protein concentrations at pH 7.4

groups. The results indicated that  $[\text{Cd}=\text{O}]$  and  $[\text{Cd}\equiv\text{N}]$  units were probably formed in the Cd–HSA complexes. Additional evidence to support the Cd interaction with C–N and N–H groups came from the shifting of the protein amide A band at  $3,312\text{ cm}^{-1}$  (N=H stretching mode) in the free HSA to  $3,304$  upon metal ion–protein complexation (spectra not shown).

Moreover, since the secondary structures are stabilized by hydrogen bonds between amide C=O and N–H groups, the position and the area of the components could reflect the patterns and the strength of the hydrogen bonds (Byler and Susi 1986). Thus, the infrared self deconvolution with second derivative resolution enhancement and curve-fitting procedures was further applied to determine the protein secondary structure changes in the absence and presence of Cd(II). A quantitative analysis of the protein secondary structure for the free HSA and its Cd cation adducts in hydrated films were carried out, and the calculated results are listed in Table 4. According to Fig. 8a and Table 4, the free HSA has 58.12 %  $\alpha$ -helix ( $1,651\text{ cm}^{-1}$ ), 13.35 %  $\beta$ -sheet ( $1,627$  and  $1,616\text{ cm}^{-1}$ ), 12.72 % turn structure ( $1,674$  and  $1,663\text{ cm}^{-1}$ ), 2.75 %  $\beta$ -antiparallel ( $1,684\text{ cm}^{-1}$ ), and 13.06 % random coil ( $1,640\text{ cm}^{-1}$ ). The results are consistent with the spectroscopic studies of human serum albumin previously reported (Beauchemin et al. 2007; Belatik et al. 2012). Upon Cd(II) interaction, an obvious decrease of  $\alpha$ -helix from 58.12 % (free HSA) to 43.43 % (1 mM Cd(II)), 39.84 % (2 mM Cd(II)), and 32.14 % (10 mM Cd(II)) with an alteration in  $\beta$ -sheet from 13.35 % (free HSA) to 14.58 % (1 mM Cd(II)), 14.79 % (2 mM Cd(II)), and 10.39 % (10 mM Cd(II)) was observed. It was noted that a remarkable increase was observed for the random coil from 13.06 % (free HSA) to 19.86 % (1 mM Cd(II)), 20.44 % (2 mM Cd(II)), and 33.28 % (10 mM Cd(II)). The content of turn structure in HSA also increases from 12.72 % (free HSA) to approximately 20 % (1, 2, 10 mM Cd(II)) in the presence of Cd. Besides, a slight structural changes of  $\beta$ -antiparallel was also observed from 2.75 (free HSA) to 4.76 % (10 mM Cd(II)). Figure 9 clearly shows that some  $\alpha$ -helix can be obviously converted into random coil when HSA is conjugated with Cd(II). The major decrease in  $\alpha$ -helix structure and increase in random coil structures suggested a partial protein unfolding with the increase of Cd(II) concentration.

Besides, in order to examine the influence of the metal ion–protein binding interaction on the hydrophobic regions of HSA, the spectral changes of HSA antisymmetric and symmetric  $\text{CH}_2$  stretching vibrations in the region of  $2,850\text{--}3,000\text{ cm}^{-1}$  were also monitored by infrared spectroscopy. As shown in Fig. 10, the  $\text{CH}_2$  bands of the free HSA located at  $2,961$ ,  $2,938$ , and  $2,876\text{ cm}^{-1}$  changed to  $2,960$ ,  $2,939$ ,  $2,901$ ,  $2,875$ ,  $2,867$ , and  $2,856\text{ cm}^{-1}$  in Cd(II)–HSA complex. The alterations of the protein antisymmetric and symmetric  $\text{CH}_2$  stretching vibrations suggested that the microenvironment of hydrophobic regions in HSA was changed through the metal ion–protein complexation.

**Table 4** Secondary structure analysis (infrared spectra) for free HSA and its Cd(II) complexes in hydrated film at pH 7.4

Amide I components (cm <sup>-1</sup> )	Secondary structure analysis (%)				Fitting peak position (cm <sup>-1</sup> )			
	HSA only	Cd(II)-HSA 1 mM	Cd(II)-HSA 2 mM	Cd(II)-HSA 10 mM	HSA only	Cd(II)-HSA 1 mM	Cd(II)-HSA 2 mM	Cd(II)-HSA 10 mM
1,692–1,680 β-anti	2.75	2.32	2.21	4.76	1,684	1,682	1,682	1,679
1,680–1,660 turn	12.72	19.81	22.72	19.43	1,672	1,663 1,674	1,663 1,675	1,666
1,660–1,650 α-helix	58.12	43.43	39.84	32.14	1,655	1,651	1,650	1,653
1,648–1,641 random coil	13.06	19.86	20.44	33.28	1,640	1,637	1,636	1,637
1,640–1,610 β-sheet	13.35	14.58	14.79	10.39	1,622 1,631	1,616 1,627	1,618 1,627	1,622

Investigation on the aggregation structural changes of HSA

In order to further confirm the aggregation state of HSA due to the addition of Cd(II), we performed DLS experiments at pH=7.4 with different molar ratios of Cd(II) to HSA to measure normalized hydrodynamic diameter (*d<sub>H</sub>*), which could give us an estimate regarding the average size of the total protein. Figure 11 represents *d<sub>H</sub>* distribution plot of HSA in the absence and presence of Cd(II). The *d<sub>H</sub>* of HSA alone in buffer was found to be around 5.16 nm (i.e., the hydrodynamic radius=2.58 nm) at pH 7.4. The *d<sub>H</sub>* values for HSA increased to 5.67 and 6.56 nm at [Cd(II)]/[HSA]=100:1 and 300:1, respectively. The increase in *d<sub>H</sub>* indicated that Cd(II) was assembled around HSA via the binding interaction between Cd(II) and HSA, leading the particle size of HSA aggregated to become larger. This result indicated that loss of charge from the binding site of albumin by the charged Cd(II) ions gave rise to dipole interaction which acted as the major contributor to promote protein aggregation. But the obvious reduce of *d<sub>H</sub>*

value to 3.81 nm happened at [Cd(II)]/[HSA]=1,000:1, which demonstrated that HSA suffered a maximum loss of its secondary structure and the conformation of HSA might be completely destroyed when Cd(II) was overdosed into the Cd(II)-HSA aqueous system. The results indicated that the presence of Cd(II) with low concentration could cause the formation of Cd(II)-HSA complex and further induce the aggregation structure changes of HSA, but Cd(II) with high concentration could result in structural damage of protein, leading to the size reduction of HSA aggregates.

Conclusion

In this work, the molecular mechanism involved in the interaction between Cd(II) and HSA was comprehensively investigated by a series of spectroscopic methods. Meanwhile, we also systematically studied the effect of food contaminant Cd(II) on the conformational stability of HSA in an aqueous environment. XPS analysis revealed the direct interaction of

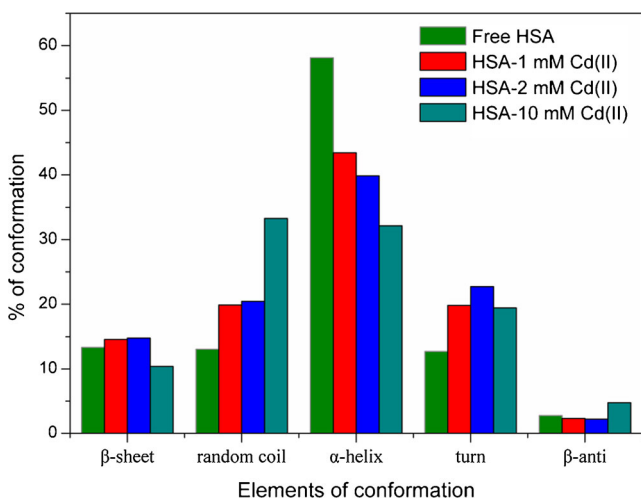


**Fig. 9** Bar diagrams of different conformations (obtained from fitted data of FTIR deconvolution) of free HSA and Cd(II)-HSA complex with fitted protein concentration  $0.2 \times 10^{-3} \text{ mol L}^{-1}$

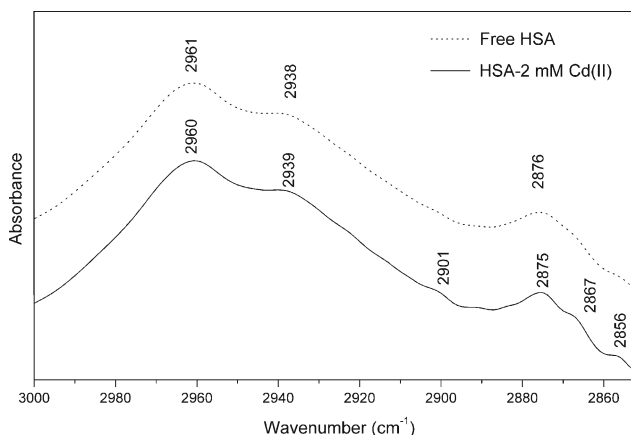


**Fig. 10** Infrared spectra of protein CH<sub>2</sub> symmetric and antisymmetric stretching vibrations and its Cd(II)-HSA complexes in the region 3,000–2,850 cm<sup>-1</sup>. The contribution of the CH stretching vibrations of the polyphenolic compounds in the region 3,000–2,850 cm<sup>-1</sup> is subtracted

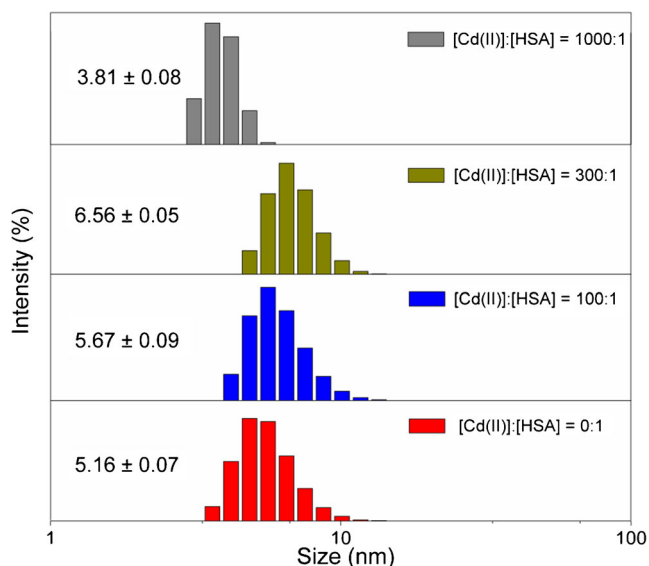


**Fig. 11** Dynamic laser light scattering spectra of HSA in the absence and presence of Cd(II) with different ion/protein molar ratio at pH 7.4. Conditions:  $[HSA]=2.0 \times 10^{-6} \text{ mol L}^{-1}$

polypeptide C, N, and O atoms of HSA with Cd(II), which induced the microenvironmental changes around these protein atoms. The fluorescence results indicated that the probable mechanism of Cd–HSA interaction is a static quenching process and the binding reaction is spontaneous. Thermodynamic analysis combined with molecular docking results showed that Cd(II) mainly interacted with the negatively charged amino acid residues Asp 451 and Gln 221 predominately through electrostatic force. The structural analysis according to FTIR suggested that with the increased amount of Cd(II), the secondary structure of HSA underwent a decrease in  $\alpha$ -helix and an increase in random coil structures. The aggregation states of HSA in the absence and presence of Cd(II) were further studied by DLS methods, and the results indicated that Cd(II) might interact with HSA and assembled around HSA, leading to the formation of HSA aggregates with larger size. However, Cd(II) with extremely high concentration could lead to the structural damage of the protein, leading to the size reduction of HSA aggregates. The basic information received from this work not only is helpful in clarifying the binding mechanism of Cd(II), the potential carcinogen, with HSA in vivo for further understanding its transportation, metabolism, elimination, and biodistribution during the blood transportation process but also will be of great importance in the toxicological evaluation of exogenous molecules at molecular level.

**Acknowledgments** The authors gratefully acknowledge the financial supports from the National Natural Science Foundation of China (no. 20875055); the Natural Science Foundation of Fujian Province, China (no. 2013J01388); the State Key Lab of Structural Chemistry, Fujian Institute of Research on the Structure of Matter; and the Opening Research Foundation of Key Laboratory of Biomedical Material in Tianjin city.

## References

- Beauchemin R, N'soukpoe-Kossi CN, Thomas TJ, Thomas T, Carpentier R, Tajmir-Riahi HA (2007) Polyamine analogues bind human serum albumin. *Biomacromolecules* 8:3177–3183
- Belatik A, Hotchandani S, Carpentier R, Tajmir-Riahi HA (2012) Locating the binding sites of Pb(II) Ion with human and bovine serum albumins. *Plos One* 7:e36723
- Byler DM, Susi H (1986) Examination of the secondary structure of proteins by deconvolved FTIR spectra. *Biopolymers* 25:469–487
- Carter DC, Ho JX (1994) Structure of serum-albumin. *Adv Protein Chem* 45(45):153–203
- Chi ZX, Liu RT (2011) Phenotypic characterization of the binding of tetracycline to human serum albumin. *Biomacromolecules* 12:203–209
- Curry S, Mandelkew H, Brick P, Franks N (1998) Crystal structure of human serum albumin complexed with fatty acid reveals an asymmetric distribution of binding sites. *Nat Struct Biol* 5:827–835
- Ding F, Wei L, Diao JX, Sun Y (2011) Characterization of alizarin Red S binding sites and structural changes on human serum albumin: a biophysical study. *J Hazard Mater* 186:352–359
- Dudka S, Adriano DC (1997) Environmental impacts of metal ore mining and processing: a review. *J Environ Qual* 26:590–602
- Feki-Tounsi M, Olmedo P, Gil F, Khelifi R, Mhiri MN, Rebai A, Hamza-Chaffai A (2013) Cadmium in blood of Tunisian men and risk of bladder cancer: interactions with arsenic exposure and smoking. *Environ Sci Pollut R* 20:7204–7213
- Flick DF, Kraybill HF, Dimitroff JM (1971) Toxic effects of cadmium—review. *Environ Res* 4:71–85
- Friberg L (1984) Cadmium and the kidney. *Environ Health Persp* 54:1–11
- Gautier A, Kirkpatrick JP, Nietlispach D (2008) Solution-state NMR spectroscopy of a seven-helix transmembrane protein receptor: backbone assignment, secondary structure, and dynamics. *Angewandte Chemie-International Edition* 47:7297–7300
- Godt J, Scheidig F, Grosse-Siestrup C, Esche V, Brandenburg P, Reich A, Groneberg DA (2006) The toxicity of cadmium and resulting hazards for human health. *J Occup Med Toxicol* 1:22
- Gu Q, Kenny JE (2009) Improvement of inner filter effect correction based on determination of effective geometric parameters using a conventional fluorimeter. *Anal Chem* 81:420–426
- Haddam N, Samira S, Dumont X, Taleb A, Lison D, Haufroid V, Bernard A (2011) Confounders in the assessment of the renal effects associated with low-level urinary cadmium: an analysis in industrial workers. *Environ Health-Glob* 10
- Hallenbeck WH (1984) Human health-effects of exposure to cadmium. *Experientia* 40:136–142
- Haq R, Zaidi SK, Shakoori AR (1999) Cadmium resistant *Enterobacter cloacae* and *Klebsiella* sp isolated from industrial effluents and their possible role in cadmium detoxification. *World J Microb Biot* 15: 283–290
- He XM, Carter DC (1992) Atomic-structure and chemistry of human serum-albumin. *Nature* 358:209–215
- Heo DH, Baek IJ, Kang HJ, Kim JH, Chang M, Jeong MY, Kim TH, Choi ID, Yun CW (2010) Cadmium regulates copper homeostasis by inhibiting the activity of Mac1, a transcriptional activator of the copper regulon, in *Saccharomyces cerevisiae*. *Biochem J* 431:257–265
- Kamal JKA, Zhao L, Zewail AH (2004) Ultrafast hydration dynamics in protein unfolding: human serum albumin. *Proc Natl Acad Sci U S A* 101:13411–13416
- Kong J, Yu S (2007) Fourier transform infrared spectroscopic analysis of protein secondary structures. *Acta Bioch Bioph Sin* 39:549–559
- Kumar A, Pastore P (2007) Lead and cadmium in soft plastic toys. *Curr Sci India* 93:818–822
- Kumar CV, Buranaprapuk A, Sze HC, Jockusch S, Turro NJ (2002) Chiral protein scissors: high enantiomeric selectivity for binding

- and its effect on protein photocleavage efficiency and specificity. *Proc Natl Acad Sci U S A* 99:5810–5815
- Lakowicz JR (2006) Principles of fluorescence spectroscopy. Springer, New York, pp 278–290
- Liu Y, Chen MM, Luo ZP, Lin JJ, Song L (2013a) Investigation on the site-selective binding of bovine serum albumin by erlotinib hydrochloride. *J Biomol Struct Dyn* 31:1160–1174
- Liu Y, Lin JJ, Chen MM, Song L (2013b) Investigation on the interaction of the toxicant, gentian violet, with bovine hemoglobin. *Food Chem Toxicol* 58:264–272
- Mandal P, Ganguly T (2009) Fluorescence spectroscopic characterization of the interaction of human adult hemoglobin and two isatins, 1-methylisatin and 1-phenylisatin: a comparative study. *J Phys Chem B* 113:14904–14913
- Mantsch HH, Chapman D (1996) Infrared spectroscopy of biomolecules. Wiley-Liss, New York, 359pp
- Mclamore ES, Zhang W, Porterfield DM, Banks MK (2010) Membrane-aerated biofilm proton and oxygen flux during chemical toxin exposure. *Environ Sci Technol* 44:7050–7057
- Mockaitis G, Rodrigues JAD, Foresti E, Zaiat M (2012) Toxic effects of cadmium (Cd<sup>2+</sup>) on anaerobic biomass: kinetic and metabolic implications. *J Environ Manage* 106:75–84
- Nursita AI, Singh B, Lees E (2009) Cadmium bioaccumulation in *Proisotoma minuta* in relation to bioavailability in soils. *Ecotoxicol Environ Saf* 72:1767–1773
- Perkins DJ (1961) Studies on the interaction of zinc, cadmium and mercuric ions with native and chemically modified human serum albumin. *Biochem J* 80:668–672
- Peters T (1985) Serum-albumin. *Adv Protein Chem* 37:161–245
- Qu SS, Liu Y, Wang TZ, Gao WY (2002) Thermodynamics of binding of cadmium to bovine serum albumin. *Chemosphere* 46:1211–1214
- Rao MSN, Lal H (1958) Metal protein interactions in buffer solutions. 2. A polarographic study of the interaction of Zn-II and Cd-II with bovine serum albumin. *J Am Chem Soc* 80:3222–3226
- Reshetin VP, Kazazyan VI, Regens JL, Gunter JT (2003) Cancer risk assessment and ambient cadmium concentrations: mortality estimates from Moscow, Samara, and Saratov. *Environ Sci Pollut R*: 162–164
- Ross PD, Subramanian S (1981) Thermodynamics of protein association reactions—forces contributing to stability. *Biochemistry* 20:3096–3102
- Sadler PJ, Viles JH (1996) <sup>1</sup>H and <sup>113</sup>Cd NMR investigations of Cd(2+) and Zn(2+) binding sites on serum albumin: competition with Ca(2+), Ni(2+), Cu(2+), and Zn(2+). *Inorg Chem* 35:4490–4496
- Scott BJ, Bradwell AR (1983) Identification of the serum binding-proteins for iron, zinc, cadmium, nickel, and calcium. *Clin Chem* 29:629–633
- Sudlow G, Birkett DJ, Wade DN (1975) The characterization of two specific drug binding sites on human serum albumin. *Mol Pharmacol* 11:824–832
- Wang Y, Yu HY, Shi XL, Luo ZP, Lin DH, Huang MD (2013) Structural mechanism of ring-opening reaction of glucose by human serum albumin. *J Biol Chem* 288:15980–15987
- Ware WR (1975) Photophysics of exciplexes—some kinetic aspects. *Pure Appl Chem* 41:635–660
- Wu B, Mu CD, Zhang GZ, Lin W (2009) Effects of Cr<sup>3+</sup> on the structure of collagen fiber. *Langmuir* 25:11905–11910
- Yang H, Huo X, Yekeen TA, Zheng QJ, Zheng MH, Xu XJ (2013) Effects of lead and cadmium exposure from electronic waste on child physical growth. *Environ Sci Pollut R* 20: 4441–4447